HEAT TRANSFER AUGMENTATION OF MAGNETOHYDRODYNAMICS NATURAL CONVECTION IN L-SHAPED CAVITIES UTILIZING NANOFLUIDS

by

Ehsan SOURTIJI * ***and Seyed Farid HOSSEINIZADEH***
Department of Mechanical Engineering, Babol University of Technology, Babol, Mazandaran, Iran

Original scientific paper
DOI: 102298/TSCI1202489S

A numerical study of natural convection heat transfer through an alumina-water nanofluid inside L-shaped cavities in the presence of an external magnetic field is performed. The study has been carried out for a wide range of important parameters such as Rayleigh number, Hartmann number, aspect ratio of the cavity and solid volume fraction of the nanofluid. The influence of the nanoparticle, buoyancy force and the magnetic field on the flow and temperature fields have been plotted and discussed. The results show that after a critical Rayleigh number depending on the aspect ratio, the heat transfer in the cavity rises abruptly due to some significant changes in flow field. It is also found that the heat transfer enhances in the presence of the nanoparticles and increases with solid volume fraction of the nanofluid. In addition, the performance of the nanofluid utilization is more effective at high Rayleigh numbers. The influence of the magnetic field has been also studied and deduced that it has a remarkable effect on the heat transfer and flow field in the cavity that as the Hartmann number increases the overall Nusselt number is significantly decreased specially at high Rayleigh numbers.

Key words: *magnetohydrodynamics, natural convection, L-shaped cavities, nanofluid*

Introduction

One of the relevant ways to enhance the heat transfer is by adding solid nanoparticles with high thermal conductivity in the fluid. The resulting fluid is a suspension of the solid nanoparticle in the base fluid which is called a "nanofluid". There are some mechanisms which explain the enhancement of thermal conductivity in nanofluids such as interfacial layer at the particle/liquid interface [1, 2], Brownian motion of the particles [3, 4], nanoparticles clustering [5], temperature and nanoparticles size and shape [6]. The utilization of the nanofluids as a convenient way to access the better performance of systems has been investigated by numerous researchers in the past several years [7-10]. Jou *et al.* [11] studied the influence of nanofluids on natural convection heat transfer in 2-D square enclosures. The transport equations were modeled using a stream function-vorticity formulation and solved by finite volume methodology. The effects of Rayleigh number and aspect ratio of the enclosure were considered and it was deduced that an enhancement in heat transfer is achieved by adding the nanoparticles to the base

* Corresponding author; e-mail: Sourtiji@yahoo.com

fluid. Abu-nada *et al.* [12] investigated numerically the effect of Cu-water nanofluid on natural convection heat transfer in an inclined cavity. They used the inclination angle as a control parameter for flow and heat transfer in the cavity and studied the problem in various inclination angle, Rayleigh numbers and solid volume fractions and found that the effect of the nanoparticles on Nusselt number is more pronounced at low volume fraction that at high volume fraction. Khanafer *et al.* [13] performed a numerical study of laminar natural convection in a square cavity. They have used three theoretical models for prediction of viscosity and thermal conductivity of nanofluids and deduced that the variances within different models have substantial effects on the results. They also found that the heat transfer increases with solid volume fraction of the nanofluid. Tiwari *et al.* [14] studied numerically combined convection heat transfer and fluid flow inside a two-sided lid-driven differentially heated square cavity for various Richardson number and the direction of the moving walls. They observed that the nanoparticles when immersed in a fluid enhances the heat transfer capacity of the base fluid and are able to alter the pattern of the flow field. Ghasemi *et al.* [15] performed a numerical study of natural convection of water-Al_2O_3 nanofluid in an enclosure subjected to an external magnetic field. They concluded that the heat transfer rate increases with an increase of the Rayleigh number but it decreases with an increase of the Hartmann number. Moreover the increment of the nanofluid volume fraction leads to enhancement or deterioration of the heat transfer performance depending on the value of Hartmann and Rayleigh numbers.

Recently, an increasing number of studies have been conducted on free convection in non-square geometries because of its wide applications in engineering and industry [16-19]. Younsi [20] presented a numerical simulation of free-convection in a trapezoidal porous cavity subjected to an axial magnetic field. It was found that the application of the transverse magnetic field normal to the flow direction decreases the Nusselt and Sherwood number. Koca *et al.* [21] investigated the influence of Parndtl number on natural convection in triangular enclosures with localized heating from below. They observed that the variation of the Prandtl number affects both the flow and temperature fields in the enclosure. In addition, it was found that the heat transfer rate increases with the increasing of Prandtl and Rayleigh numbers for all cases.

In the present study the effect of magnetic field on natural convection heat transfer of water-based Al_2O_3 nanofluids inside L-shaped cavities is investigated numerically. For this purpose various combinations of Rayleigh number, Hartmann number, aspect ratio of the L-shaped cavities, and volume fraction of the Al_2O_3 solid nanoparticles are considered. Furthermore the model presented by Murshed *et al.* [2], is used to simulate the presence of the nanoparticles in the base fluid.

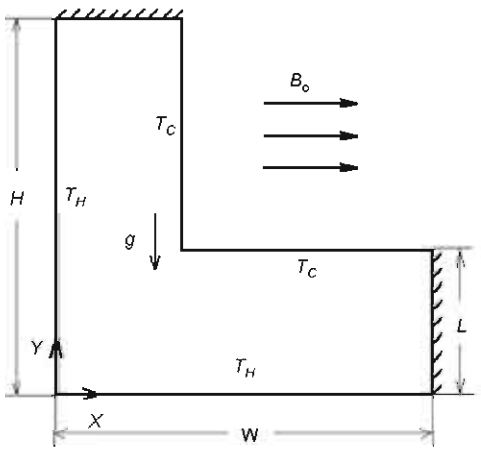

Figure 1. Schematic diagram of the L-shaped cavity with an external magnetic field

Problem formulation

The schematic drawing of the system and co-ordinates are shown in fig. 1. The height and width of the cavity are denoted by H and W respectively with $H = W$. The thickness of the cavity is shown by L, and the aspect ratio of the cavity is specified by $AR = L/H$. The depth of

the enclosure perpendicular to the plane of the diagram is assumed to be long. Hence, the problem can be considered to be 2-D. The uniform magnetic field with a constant magnitude of B_o is considered in the horizontal direction. The cavity is filled with Al_2O_3-water (Pr = 6.2), and the physical properties of the fluid are assumed to be constant except for the density which is estimated by the Boussinesq's approximation. The thermophysical properties of the fluid phase and the nanoparticles at $T = 250$ are presented in tab. 1. With these assumptions the dimensional conservation equations are as follows:

– continuity

$$\frac{\partial u}{\partial x}+\frac{\partial v}{\partial y}=0 \tag{1}$$

– momentum

$$u\frac{\partial u}{\partial x}+v\frac{\partial u}{\partial y}=-\frac{1}{\rho_{\mathrm{nf}}}\frac{\partial P}{\partial x}+\frac{\mu_{\mathrm{nf}}}{\rho_{\mathrm{nf}}}\left(\frac{\partial^2 u}{\partial x^2}+\frac{\partial^2 u}{\partial y^2}\right) \tag{2}$$

$$u\frac{\partial v}{\partial x}+v\frac{\partial v}{\partial y}=-\frac{1}{\rho_{\mathrm{nf}}}\frac{\partial P}{\partial y}+\frac{\mu_{\mathrm{nf}}}{\rho_{\mathrm{nf}}}\left(\frac{\partial^2 v}{\partial x^2}+\frac{\partial^2 v}{\partial y^2}\right)+\frac{(\rho\beta)_{\mathrm{nf}}}{\rho_{\mathrm{nf}}}\mathrm{g}(T-T_{\mathrm{C}})-\frac{\sigma_{\mathrm{nf}}B_0^2 v}{\rho_{\mathrm{nf}}} \tag{3}$$

– energy

$$u\frac{\partial T}{\partial x}+v\frac{\partial T}{\partial y}=\alpha_{\mathrm{nf}}\left(\frac{\partial^2 T}{\partial x^2}+\frac{\partial^2 T}{\partial y^2}\right) \tag{4}$$

where $\alpha_{\mathrm{nf}} = k_{\mathrm{nf}}/(\rho c_p)_{\mathrm{nf}}$.

The density and electrical conductivity of the nanofluid are given by:

$$\rho_{\mathrm{nf}} = (1-\varphi)\rho_{\mathrm{f}} = \varphi\rho_{\mathrm{P}} \tag{5}$$

$$\sigma_{\mathrm{nf}} = (1-\varphi)\sigma_{\mathrm{f}} = \varphi\sigma_{\mathrm{P}} \tag{6}$$

The heat capacitance of the nanofluid and part of the Boussinesq are expressed as:

Table 1. Thermophysical properties of the base fluid and the Al_2O_3 nanoparticles at $T = 250$

	c_p [$Jkg^{-1}K^{-1}$]	ρ [kgm^{-3}]	k [$Wm^{-1}K^{-1}$]	$\beta\cdot10^{-5}$ [K^{-1}]
Water	4179	997.1	0.613	21
Al_2O_3	765	3970	40	0.85

$$(\rho c_p)_{\mathrm{nf}} = (1-\varphi)(\rho c_p)_{\mathrm{f}} + \varphi(\rho c_p)_{\mathrm{P}} \tag{7}$$

$$(\rho\beta)_{\mathrm{nf}} = (1-\varphi)(\rho\beta)_{\mathrm{f}} + \varphi(\rho\beta)_{\mathrm{P}} \tag{8}$$

with φ being the volume fraction of the solid nanoparticles and subscripts f, nf, and P stand for base fluid, nanofluid, and particle, respectively.

The effective viscosity of nanofluid is determined using the following relation [22]:

$$\mu_{\mathrm{nf}} = \mu_{\mathrm{f}}(1-\varphi)^{-2.5} \tag{9}$$

This is based on experimental data in the literature for Al_2O_3–water nanofluids.

The effective thermal conductivity of the nanofluid was given by Murshed *et al.* [2] as follows:

$$k_{\mathrm{nf}} = \frac{(k_{\mathrm{P}}-k_{\mathrm{lr}})\varphi_p k_{\mathrm{lr}}[2\beta_1^3-\beta^3+1]+(k_p+2k_{\mathrm{lr}})\beta_1^3[\varphi_p\beta^3(k_{\mathrm{lr}}-k_{\mathrm{f}})+k_{\mathrm{f}}]}{\beta_1^3(k_p+2k_{\mathrm{lr}})-(k_p k_{\mathrm{lr}})\varphi_p[\beta_1^3+\beta^3-1]} \tag{10}$$

with $1+h/a=\beta$, $1+h/2a=\beta_1$, and, $k_{\mathrm{lr}}=2k_{\mathrm{f}}$. Here, h is the interfacial layer thickness, a – the particle radius, and subscript lr denote the interfacial layer. Note that for the case of a particle-free fluid ($\varphi = 0$), the above relations transform into their typical forms.

Dimensionless form of the governing equations can be obtained via introducing dimensionless variables as follow:

$$X=\frac{x}{H},\ Y=\frac{y}{H},\ AR=\frac{L}{H},\ U=\frac{uH}{\alpha_{\mathrm{f}}},\ V=\frac{vH}{\alpha_{\mathrm{f}}},\ \theta=\frac{T-T_{\mathrm{C}}}{T_{\mathrm{H}}-T_{\mathrm{C}}},\ P=\frac{pH^2}{\rho_{\mathrm{f}}\alpha_{\mathrm{f}}^2}$$
$$\mathrm{Pr}=\frac{\nu_{\mathrm{f}}}{\alpha_{\mathrm{f}}},\ \mathrm{Ra}=\frac{\mathrm{g}\beta_{\mathrm{f}}H^3(T_{\mathrm{H}}-T_{\mathrm{C}})}{\nu_{\mathrm{f}}\alpha_{\mathrm{f}}},\ \mathrm{Ha}=B_{\mathrm{o}}H\sqrt{\frac{\sigma_{\mathrm{nf}}}{\rho_{\mathrm{nf}}\nu_{\mathrm{f}}}} \tag{11}$$

Based on the dimensionless variables above, the dimensionless equations for the conservation of mass, momentum, and thermal energy are as follow:

$$\frac{\partial U}{\partial X}+\frac{\partial V}{\partial Y}=0 \tag{12}$$

$$U\frac{\partial U}{\partial X}+V\frac{\partial U}{\partial Y}=-\frac{\rho_{\mathrm{f}}}{\rho_{\mathrm{nf}}}\frac{\partial P}{\partial X}+\frac{\mu_{\mathrm{nf}}}{\rho_{\mathrm{nf}}\alpha_{\mathrm{f}}}\left(\frac{\partial^2 U}{\partial X^2}+\frac{\partial^2 U}{\partial Y^2}\right) \tag{13}$$

$$U\frac{\partial U}{\partial X}+V\frac{\partial U}{\partial Y}=-\frac{\rho_{\mathrm{f}}}{\rho_{\mathrm{nf}}}\frac{\partial P}{\partial Y}+\frac{\mu_{\mathrm{nf}}}{\rho_{\mathrm{nf}}\alpha_{\mathrm{f}}}\left(\frac{\partial^2 V}{\partial X^2}+\frac{\partial^2 V}{\partial Y^2}\right)+$$
$$+\frac{\varphi\rho_{\mathrm{P}}\beta_{\mathrm{P}}+(1-\varphi)\rho_{\mathrm{f}}\beta_{\mathrm{f}}}{\rho_{\mathrm{nf}}\beta_{\mathrm{f}}}\mathrm{Ra}\,\mathrm{Pr}\,\theta-\mathrm{Ha}^2\mathrm{Pr}V \tag{14}$$

$$U\frac{\partial\theta}{\partial X}+V\frac{\partial\theta}{\partial Y}=\frac{\alpha_{\mathrm{nf}}}{\alpha_{\mathrm{f}}}\left(\frac{\partial^2\theta}{\partial X^2}+\frac{\partial^2\theta}{\partial y^2}\right) \tag{15}$$

In the energy equation, the viscous dissipation terms are neglected and parameters α and ν are the thermal diffusivity and kinematic viscosity of the fluid, respectively.

The dimensionless forms of the boundary conditions are:

$$U(X,1)=U(X,AR)=U(X,0)=0,\quad U(0,Y)=U(1,Y)=U(AR,Y)=0,$$
$$V(X,1)=V(X,AR)=V(X,0)=0,\quad V(0,Y)=V(1,Y)=V(AR,Y)=0,$$
$$\theta(X,0)=1,\quad \theta(X,AR)\big|_{X>AR}=0,\quad \frac{\partial\theta(X,1)}{\partial Y}\bigg|_{X<AR}=0,$$
$$\theta(0,Y)=1,\quad \theta(AR,Y)\big|_{Y>AR}=0,\quad \frac{\partial\theta(1,Y)}{\partial X}\bigg|_{Y<AR}=0. \tag{16}$$

In order to evaluate the heat transfer enhancement in the cavity, the local Nusselt number on the walls is defined as:

$$\mathrm{Nu}_{\mathrm{l}}=-\frac{k_{\mathrm{nf}}}{k_{\mathrm{f}}}\frac{\partial\theta}{\partial n}\bigg|_{\mathrm{wall}} \tag{17}$$

The symbol n is the normal direction to the surface. The average Nusselt number along the hot walls of the cavity is considered to evaluate the overall heat transfer rate and is defined as follow:

$$\mathrm{Nu}_{\mathrm{avg}}=\frac{1}{2}\left(\int_{Y=0}^{1}-\frac{k_{\mathrm{nf}}}{k_{\mathrm{f}}}\frac{\partial\theta}{\partial X}\bigg|_{X=0}+\int_{X=0}^{1}-\frac{k_{\mathrm{nf}}}{k_{\mathrm{f}}}\frac{\partial\theta}{\partial Y}\bigg|_{Y=0}\right) \tag{18}$$

Computational details

The governing equations were iteratively solved by the finite-volume-method using Patankar's SIMPLE algorithm [23]. A 2-D 80 × 80 uniformly spaced staggered grid system was used. The QUICK scheme was utilized for the convective terms, whereas the central difference scheme was used for the diffusive terms. The under-relaxation factors for the velocity components, pressure correction, and thermal energy are all set to 0.2. Tolerance of the normalized residuals upon convergence is set to 10^{-6} for all cases.

The validation of the code was done by comparing the average Nusselt number computed by the present code results with those of M. Mahmoodi [19] for natural convection heat transfer of Cu-water nanofluid inside the L-shaped cavity as shown in fig. 2 and a good agreement is observed. Note that in order to have a proper comparison, we used the same models for prediction of the effective viscosity and thermal conductivity of nanofluids.

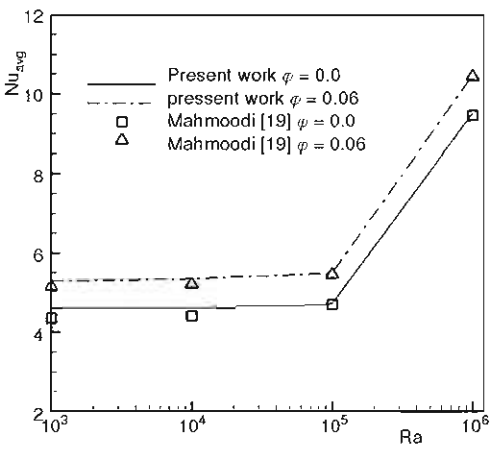

Figure 2. The average Nusselt number of Cu-water filled L-shaped cavity with AR = 0.2 computed by the present study and Mahmoodi [19]

Results and discussions

As mentioned before, the main purpose of this study is to investigate numerically the effects of adding nanoparticles to the base fluid and the presence of an external magnetic field on the flow and heat transfer in natural convection inside L-shaped cavities. The effect of magnetic field is evaluated using a dimensionless number called Hartmann number. The study is performed for various combinations of Rayleigh number, Hartmann number, aspect ratio of the L-shaped cavity, and volume fraction of the solid nanoparticles.

Figure 3 illustrates variations of the streamlines inside the cavity with aspect ratio 0.2 and Rayleigh numbers from 10^3 to 10^6 in the presence of the nanoparticles and external magnetic field. It is seen that for a range of Rayleigh number from 10^3 to 10^5, a clock-wise (CW) rotating vortex occupies the vertical section of the cavity due to the buoyancy force direction. The strength of this circulation augments as the Rayleigh number increases because of the stronger buoyant flows, and diminishes as the Hartmann number increases due to the influence of the magnetic field on the convective flows. This subject is also apparent from the maximum stream function value that as the nanofluid is subjected by the magnetic field, the maximum stream function value decreases. The horizontal part of the cavity shows poor motion of the fluid. So it can be found that most of the energy is exchanged in the vertical section and the horizontal section that the conduction mechanism is the dominated mechanism in heat transfer, has lower contribution in heat exchange. For the cases with high Rayleigh number of 10^6 the buoyancy force adjacent to the hot walls is very strong, so a number of CW and counter clock wise (CCW) rotating vortices are created in the horizontal part of the cavity to make some small cycles which transfer the heat in the short distance between the two horizontal hot and cold walls. These variations in the flow field in the cavity cases to augment the convection mechanism of heat transfer

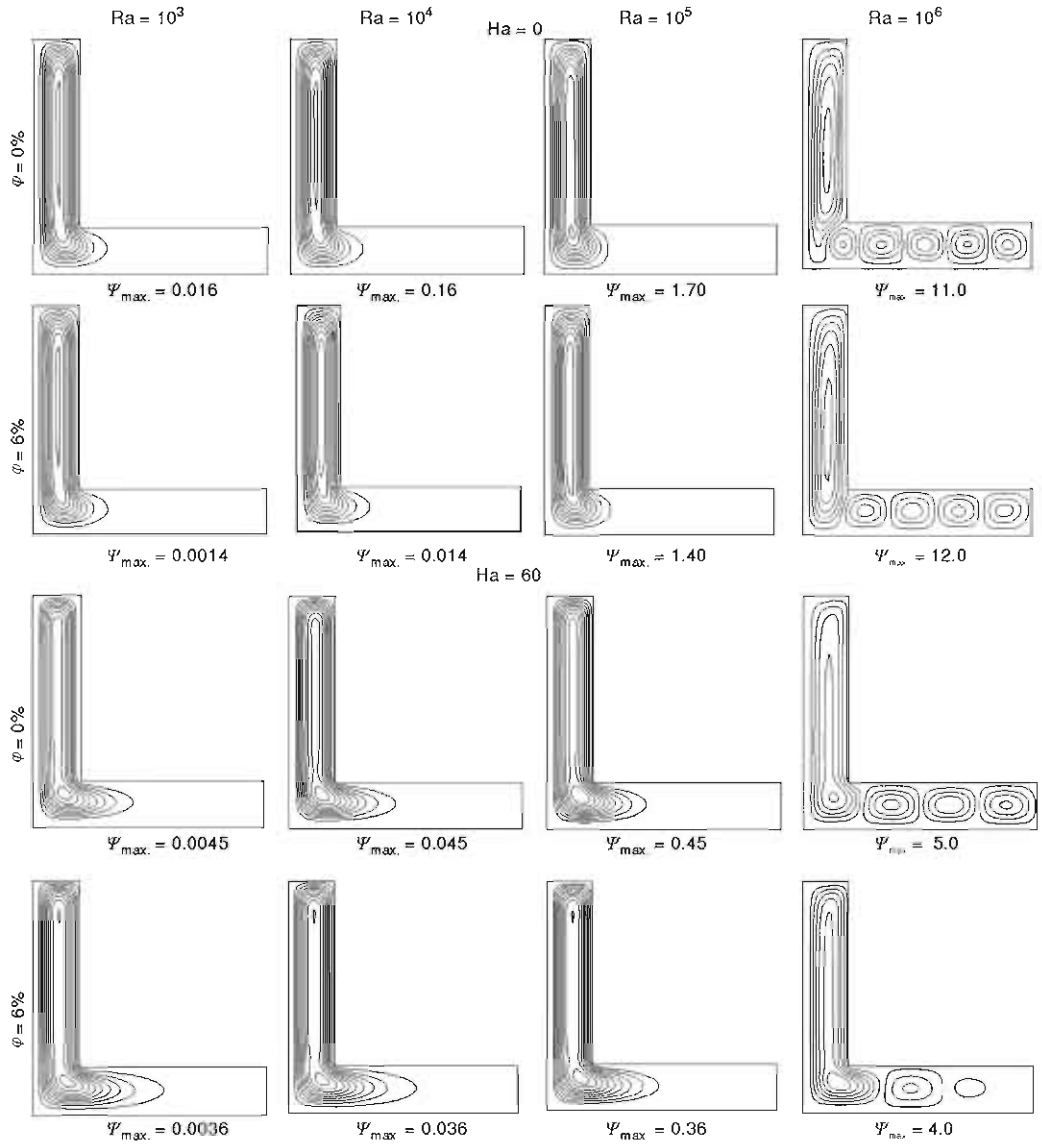

Figure 3. Variations of the streamlines inside the cavity with $AR = 0.2$ and $Ra = 10^3$-10^6 with the presence of the nanoparticles and external magnetic field

in the horizontal part of the cavity and therefore it is expected that the total heat transfer rate will be increased considerably for these cases of high Rayleigh number. It is also seen that the flow field in the cavity is affected by the presence of the nanoparticles as after adding the nanoparticles to the base fluid at a volume fraction of 0.06, the maximum stream function is decreased that shows weaker motion of the CW and CCW rotating vortices in the cavity. This decline is more sensible at low Rayleigh numbers where the conduction is the dominated mechanism. With these observations it can be deduced that the fluid flow activity in the cavity is decreased by adding the nanoparticles because of suppression of the natural convection inside

the enclosure with increase in the volume fraction of the nanoparticles and the rise in the viscosity of the nanofluid due to the clustering of the nanoparticles and size of them which are several times bigger than the molecules of the fluid and collisions between them that totally cased to raise the viscosity of the nanofluid. However in all the cases shown in fig. 3, the flow patterns in the cavity do not change considerably by adding the nanoparticles to the base fluid. The similar variations in the fluid flow are observed in figs. 4 and 5 which show the streamlines for the cavities with aspect ratio of 0.4 and 0.6 respectively at different Rayleigh and Hartmann numbers. It

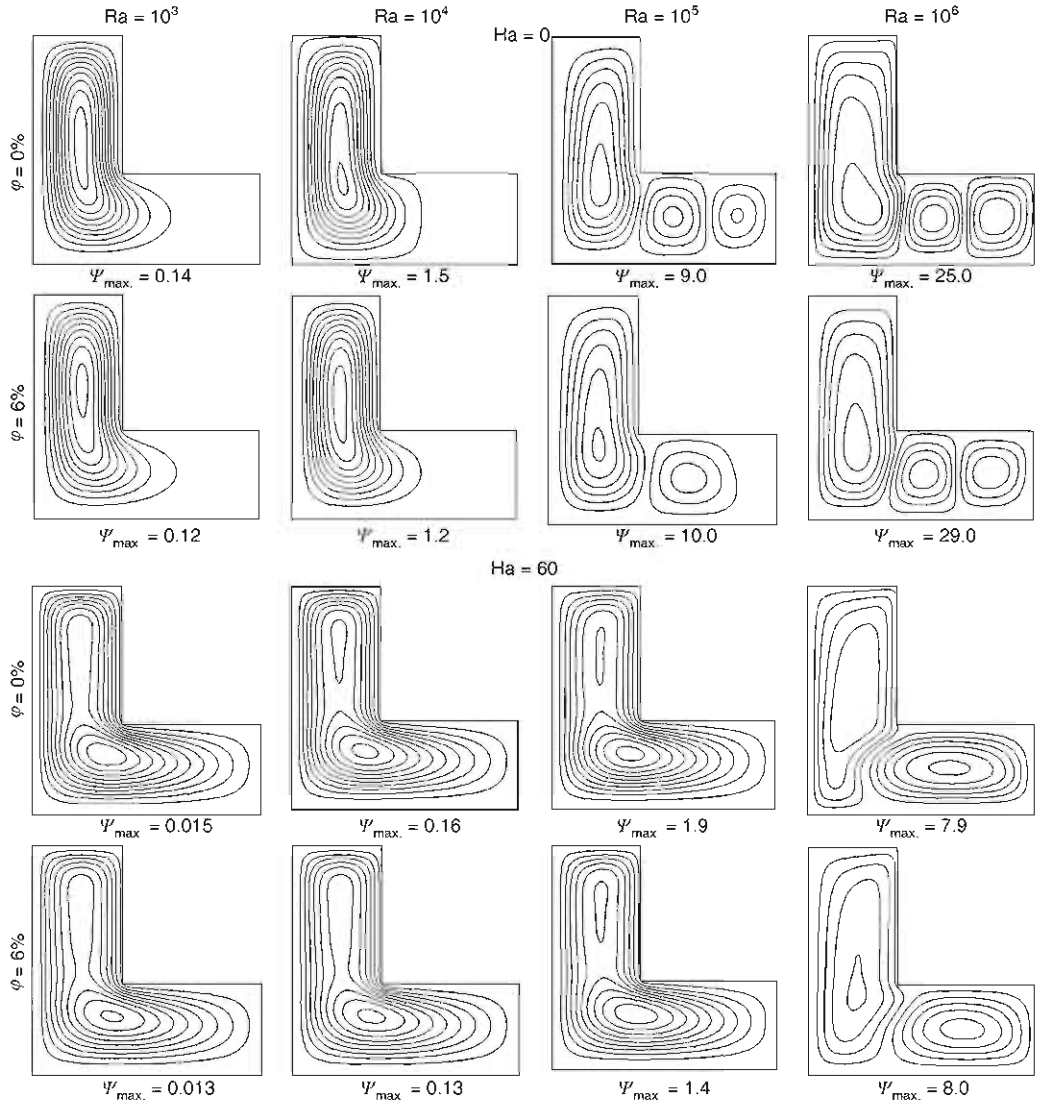

Figure 4. Variations of the streamlines inside the cavity with $AR = 0.4$ and $Ra = 10^3$-10^6 with the presence of the nanoparticles and external magnetic field

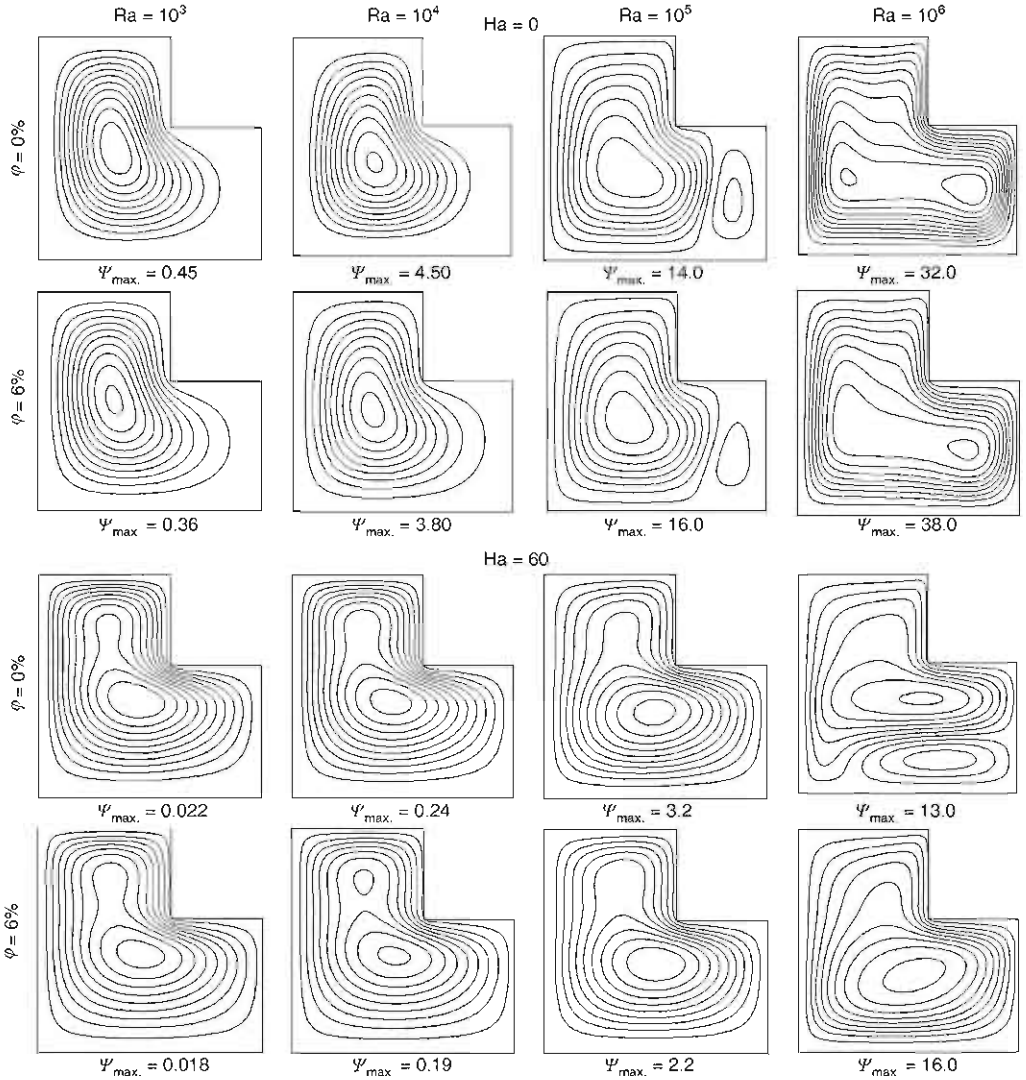

Figure 5. Variations of the streamlines inside the cavity with AR = 0.6 and Ra = 10^3-10^6 with the presence of the nanoparticles and external magnetic field

is seen that the flow field inside the cavity decays by adding the Al_2O_3 nanoparticles to the base fluid especially at low Rayleigh numbers as the maximum stream function values decay in the presence of the nanoparticles. At high Rayleigh numbers, the value of the maximum stream function is increased as a result of strengthening the buoyancy-induced flow field and it is observed that adding the nanoparticles associates with higher Rayleigh numbers where the convection flows dominate the heat transfer mechanism. As mentioned before, the external magnetic field diminishes the flow field in the cavity as the maximum stream function decreases when the Hartmann number rises. This reduction is more visible at high Rayleigh numbers. For example in the cavity of aspect ratio 0.4 at Ra = 10^5 in fig. 4, by applying the magnetic field the three CW and CCW rotating vortices are merged and form a CW rotating vortex which covers

the lower part of the cavity. The similar treatment is seen at Ra = 10^6 that the two CW and CCW vortices are united and make one CW vortex. This behavior cases to decrease the heat transfer rate and therefore it is deduced that when the Hartmann number increases the amount of heat exchange is decreased. Nevertheless for the cases with lower Rayleigh numbers (10^3 and 10^4), it is seen that however the applying magnetic field reduces the fluid motion inside the cavity but as seen specially in figs. 3 and 4, the magnetic field augments the fluid movement in the horizontal part of the cavity and therefore augments heat exchange in this part so the lesser decrease in heat transfer is expected to be seen.

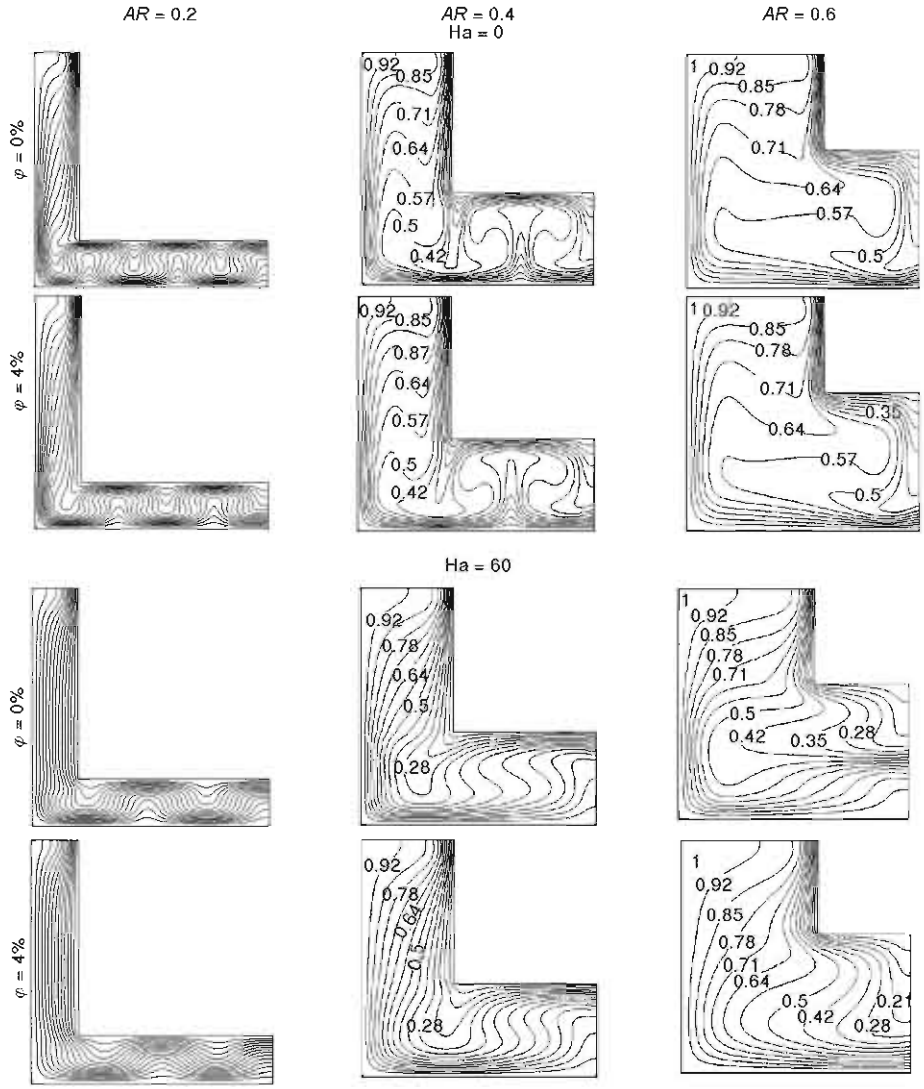

Figure 6. The effects of the nanoparticles and magnetic field on isotherm lines at Ra = 10^6 and various aspect ratios

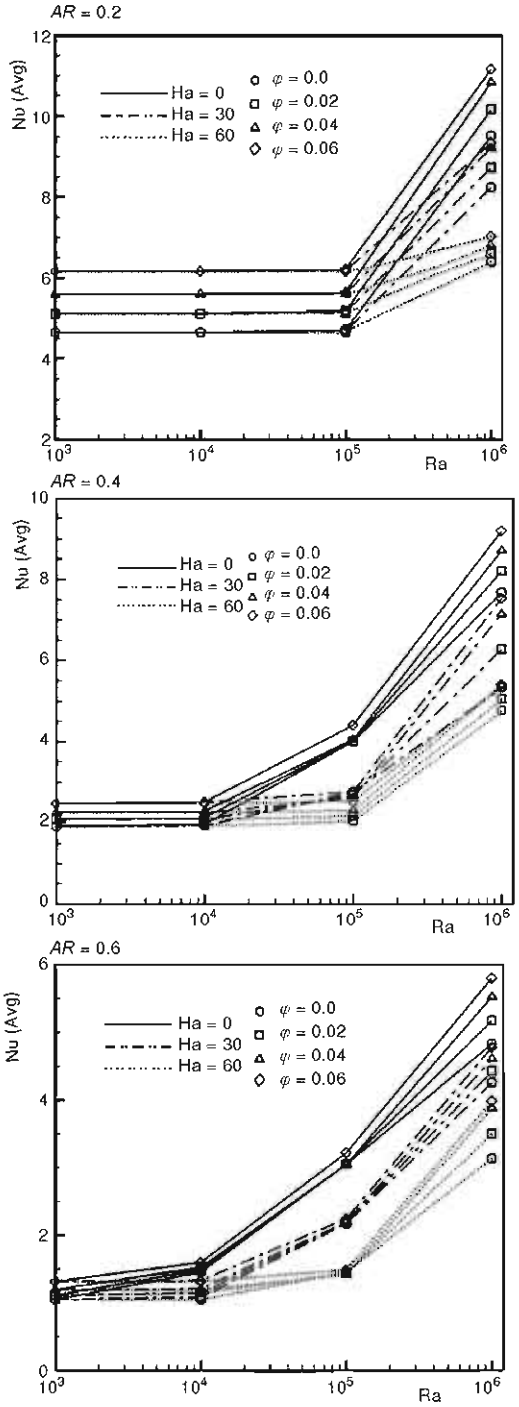

Figure 7. Variations of the average Nusselt number with Rayleigh number for different Hartman Numbers and aspect ratios

Figure 6 illustrates the isotherm lines at Rayleigh number of 10^6 and various aspect ratios in the presence of the nanoparticles and the external magnetic field. By adding the nanoparticles to the pure fluid, the thermal conductivity of the resulting fluid will be enhanced. So as seen in fig. 6, the thickness of the thermal boundary layer adjacent to the hot and cold walls of the cavity are raised due to the augmentation of the conduction mechanism of heat exchange and raising the viscosity of the fluid and the temperature gradients near the wall surfaces decreases. The influence of the applied magnetic field is illustrated in fig. 6. It is observed that as the Hartmann number increases, the isotherm lines becomes more regular and parallel flat lines with the walls of the cavity and the temperature gradients adjacent to the walls are decreased which show that the conduction mechanism is enhanced and the circulation flow in the cavity decays by applying the magnetic field. So as the Hartmann number rises, the contribution of the convection mechanism on heat exchange reduces and the temperature gradients are decreased.

Figure 7 shows variations of the average Nusselt number of the hot walls of the cavity with the solid volume fraction of the nanoparticles for various Rayleigh number, Hartmann number, and aspect ratios of the L-shaped cavity. It is clear from the figure that the average Nusselt number enhances in the presence of the nanoparticles and increases with solid volume fraction of the nanofluid. The presence of the nanoparticles in the base fluid raises the average Nusselt number by about 27.47% for Ra = 10^6, Ha = = 60, AR = 0.6, and 33% for Ra = 10^5, Ha = = 60, AR=0.2 at a volume fraction of 0.06. Figure 7 presents the results for different aspect ratios. It is seen that for the case of AR = = 0.2, the average Nusselt number remains constant as the Rayleigh number rises from 10^3 to 10^5. Then as the Rayleigh number increases from 10^5 to 10^6, a considerable en-

hancement in the average Nusselt number is observed. As mentioned in fig. 3, this is due to the formation of some CW and CCW vortices in the horizontal part and augmentation of the CW vortex in the vertical side of the cavity. In the other hand when the Rayleigh number raises from 10^5 to 10^6 the conduction dominated mechanism changes to convection mechanism. Similar situation is happened for the case of $AR = 0.4$, when the Rayleigh number grows from 10^4 to 10^5. It is also evident from the two case of $AR = 0.4$ and $AR = 0.6$ that the performance of the nanofluid at high Rayleigh number of 10^6 is more than that of lower Rayleigh numbers. Figure 7 also illustrates the influence of the applied magnetic field on the average Nusselt number for various Rayleigh numbers from 10^3 to 10^6.

It is deduced that the external magnetic field affects the heat transfer rate in the enclosure and as the Hartmann number increases the average Nusselt number of the cavity decreases. Furthermore it can be found that at low Rayleigh numbers where the heat transfer by the conduction mechanism is more important, the applied magnetic field does not have a considerable effect on the heat exchange due to the weak fluid movement inside the enclosure. At high value of the Rayleigh number, the convection mechanism has a great contribution in heat transfer and the magnetic field can suppress the flow fields in the cavity, so the average Nusselt number decreases when the Hartmann number rises. This matter is clearly seen in fig. 8. In this figure, the average Nusselt number ratio ($Nu_{avg} / Nu_{avg, Ha=0}$) has been plotted to examine the effect of the magnetic field in heat transfer for various Rayleigh numbers. The average Nusselt number in the absence of the magnetic field ($Ha = 0$) is set as the reference value and the volume fraction of the nanofluid is assumed to be constant ($\varphi = 0.04$). As observed earlier in fig. 7, the magnetic field is almost unimportant at low Rayleigh numbers that as the Hartmann number increases, the average Nusselt number ratio has inconsiderable changes and at high Rayleigh numbers, when the Hartman number raises the average Nusselt number ratio decreases.

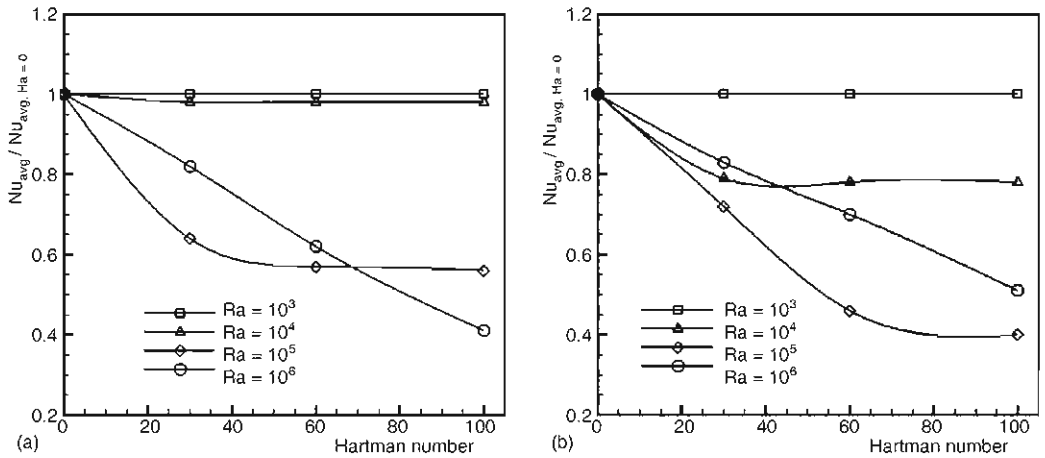

Figure 8. The influence of the magnetic field on the average Nusselt number ratio of the nanofluid for (a) AR = 0.4, (b) AR = 0.6

Conclusions

In this paper, the flow and heat transfer characteristics of alumina (Al_2O_3)-water nanofluid on natural convection heat transfer inside the L-shaped cavities in the presence of an external magnetic field have been studied numerically. For this purpose, the effects of the im-

portant parameter such as the Rayleigh number, Hartmann number, aspect ratio of the cavity and solid volume fraction of the nanofluid on the heat transfer and fluid flow inside the cavity were studied. It is found that a CW rotating vortex is the main feature of the flow field inside the cavity at low Rayleigh numbers and as the Rayleigh number grows and reaches to a critical value, the heat transfer in the cavity rises abruptly due to some significant changes in flow field. The results show that the heat transfer is augmented by adding the nanoparticles to the base fluid and increases with solid volume fraction of the nanofluid. Furthermore the performance of the nanofluid utilization is more effective at high Rayleigh numbers. The influence of the magnetic field was also studied and deduced that it has a remarkable effect on the heat transfer and flow field in the cavity that as the Hartmann number increases the overall Nusselt number is significantly decreased specially at high Rayleigh numbers.

Nomenclature

AR – aspect ratio of the L-shaped cavity, [–]
B_o – strength of the magnetic field, [T]
c_p – specific heat at constant pressure, [$Jkg^{-1}K^{-1}$]
g – gravitational acceleration, [ms^{-2}]
H – height of cavity, [m]
Ha – Hartmann number, ($= B_oL\,(\sigma_{nf}/\rho_{nf}\nu_f)^{1/2}$, [–]
k – thermal conductivity, [$Wm^{-1}K^{-1}$]
Nu – Nusselt number, [–]
P – dimensionless pressure, ($=p/\rho_{nf}u_{in}^2$)
p – pressure, [Nm^{-2}]
Pr – Prandtl number, Pr = 6.2, ($=\nu_f/\alpha_f$)
Ra – Rayleigh number, ($=g\beta\Delta\theta H^3/\nu\alpha$), [–]
T – temperature, [K]
T_H – temperature of hot left wall, [K]
T_C – temperature of hot right wall, [K]
U, V – dimensionless velocity component, ($U=u/u_0$, $V=\nu/u_0$)
u, ν – components of velocity, [ms^{-1}]
X, Y – dimensionless Cartesian co-ordinates, ($X=x/H$, $Y=y/H$)
x, y – Cartesian co-ordinates, [m]
u – velocity, [ms^{-1}]

Greek symbols

α – thermal diffusivity, [m^2s^{-1}]
β – thermal expansion coefficient, [K^{-1}]
$\underline{\theta}$ – dimensionless temperature, [–]
μ – dynamic viscosity, [Pa·s]
ν – kinematic viscosity, [m^2s^{-1}]
ρ – density, [kgm^{-3}]
σ – electrical conductivity, [μScm^{-1}]
φ – particle volume fraction, [–]
ψ – stream function, [–]

Subscripts

avg – average
f – fluid
nf – nanofluid
P – particle
lr – layer

References

[1] Yu, W., Choi, S. U. S., The Role of Interfacial Layers in the Enhanced Thermal Conductivity of Nanofluids: A Renovated Hamilton-Crosser Model, *Journal of Nanoparticle Research, 6* (2004), 4, pp. 355–361
[2] Murshed, S. M. S., Leong, K. C., Yang, C., Thermophysical and Electrokinetic Properties of Nanofluids – A Critical Review, *Applied Thermal Engineering, 28* (2008), 17-18, pp. 2109-2125
[3] Jang, S. P., Choi, S. U. S., The Role of Brownian Motion in the Enhanced Thermal Conductivity of Nanofluids, *Applied Physics Letters, 84* (2004), 21, pp. 4316-4318
[4] Murugesan, C., Sivan, S., Limits of Thermal Conductivity of Nanofluids, *Thermal Science, 14* (2010), 1, pp. 65-71
[5] Karthikeyan, N. R., Philip, J., Raj, B., Effect of Clustering on the Thermal Conductivity of Nanofluids, *Materials Chemistry and Physics, 109* (2008), 1, pp. 50-55
[6] Xuan, Y., Li, Q., Heat Transfer Enhancement of Nanofluids, *International Journal of Heat and Fluid Flow, 21* (2000), 1, pp. 58-64

[7] Abu-Nada, E., *et al.*, Effect of Nanofluid Variable Properties on Natural Convection in Enclosures, *International Journal of Thermal Sciences, 49* (2010), 3, pp. 479-491
[8] Han, W. S., Rhi, S. H., Thermal Characteristics of Grooved Heat Pipe with Hybrid Nanofluids, *Thermal Science, 15* (2011), 1, pp. 195-206
[9] Ranjbar, A. A., *et al.*, Numerical Heat Transfer Studies of a Latent Heat Storage System Containing Nano-Enhanced Phase Change Material, *Thermal Science, 15* (2011), 1, pp. 169-181
[10] Sourtiji, E., *et al.*, Effect of Water-Based Al_2O_3 Nanofluids on Heat Transfer and Pressure Drop in Periodic Mixed Convection Inside a Square Ventilated Cavity, *International Communications in Heat and Mass Transfer, 38* (2011), 8, pp. 1125-1134
[11] Jou, R. Y., Tzeng, S. C., Numerical Research of Nature Convective Heat Transfer Enhancement Filled with Nanofluids in Rectangular Enclosures, *International Communications in Heat and Mass Transfer, 33* (2006), 6, pp. 727-736
[12] Abu-Nada, E., Oztop, H. F., Effects of Inclination Angle on Natural Convection in Enclosures Filled with Cu-Water Nanofluid, *International Journal of Heat and Fluid Flow, 30* (2009), 4, pp. 669-678
[13] Khanafer, K., Vafai, K., Lightstone, M., Buoyancy-Driven Heat Transfer Enhancement in a Two-Dimensional Enclosure Utilizing Nanofluids, *International Journal of Heat and Mass Transfer, 46* (2003), 19, pp. 3639-3653
[14] Tiwari, R. K., Das, M. K., Heat Transfer Augmentation in a Two-Sided Lid-Driven Differentially Heated Square Cavity Utilizing Nanofluids, *International Journal of Heat and Mass Transfer, 50* (2007), 9-10, pp. 2002-2018
[15] Ghasemi, B., Aminossadati, S. M., Raisi, A., Magnetic Field Effect on Natural Convection in A Nanofluid-Filled Square Enclosure, *International Journal of Thermal Sciences, 50* (2011), 9, pp. 1748-1756
[16] Tasnim, S. H., Mahmud, S., Laminar Free Convection Inside an Inclined L-Shaped enclosure, *International Communications in Heat and Mass Transfer, 33* (2006), 8, pp. 936-942
[17] Dagtekin, I., Oztop, H. F., Bahloul, A., Entropy Generation for Natural Convection in Γ-Shaped Enclosures, *International Communications in Heat and Mass Transfer, 34* (2007), 4, pp. 502-510
[18] Aich, W., Hajri, I., Omri, A., Numerical Analysis of Natural Convection in a Prismatic Enclosure, *Thermal Science, 15* (2011), 2, pp. 437-446
[19] Mahmoodi, M., Numerical Simulation of Free Convection of a Nanofluid in L-Shaped Cavities, *International Journal of Thermal Sciences, 50* (2011), 9, pp. 1731-1740
[20] Younsi, R., Computational Analysis of MHD Flow, Heat and Mass Transfer in Trapezoidal Porous Cavity, *Thermal Science, 13* (2009), 1, pp. 13-22
[21] Koca, A., Oztop, H. F., Varol, Y., The Effects of Prandtl Number on Natural Convection in Triangular Enclosures with Localized Heating from Below, *International Communications in Heat and Mass Transfer, 34* (2007), 4, pp. 511-519
[22] Brinkman, H. C., The Viscosity of Concentrated Suspensions and Solution, *The Journal of Chemical Physics, 20* (1952), 4, pp. 571-581
[23] Patankar, S. V., Numerical Heat Transfer and Fluid Flow, 1st ed., Hemisphere, Washington DC, 1980

Paper submitted: November 14, 2011
Paper revised: April 27, 2012
Paper accepted: April 28, 2012